IJCRT.ORG ISSN : 2320-2882

INTERNATIONAL JOURNAL OF CREATIVE RESEARCH THOUGHTS (IJCRT)

An International Open Access, Peer-reviewed, Refereed Journal

COMPUTATIONAL INTELLIGENCE TECHNIQUE FOR CONTROL OF FACTS DEVICES FOR DEREFULATED POWER SYSTEM

[1] M.Sri Shaleni, , [2] Dr.K.Suresh
Deparatment of Power Electronics and Drives
Sri Sairam Engineering College,Chennai,India

Abstract: **This research employs Differential Evolution (DE) to find the optimal feasible placement and control of Flexible AC Transmission System (FACTS) devices in an effort to achieve Security Constrained Optimal Power Flow (SCOPF) in a deregulated energy market. SCOPF is an acronym that stands for Security-Constrained Optimal Power Flow. In this method, the AC load flow equations are modified to include constraints on power system generation, transmission line flow, bus voltage magnitude, and FACTS device settings. Two different kinds of FACTS devices, referred to as thyristor-controlled series compensators (TCSC) and static VAR compensators (SVC), are utilised in the suggested method. In order to accurately represent the bilateral exchanges, secured bilateral transaction matrices with the AC distribution factor and the slack bus contribution are utilised. The cost of installing FACTS devices under typical conditions of operation was factored into the calculation of SCOPF in this body of work. The simulation of an IEEE 6 bus system is used to test and validate the proposed method. An investigation is carried out into the economic and security implications that FACTS devices may have on bilateral transactions within a deregulated electrical grid. According to the findings, the active power production cost as well as the installation cost of FACTS devices can be decreased by determining the suitable position and control of these devices using the DE algorithm. This can also reduce the cost of bidding on the active power generated. Because SVC provides lower bids for active power generation and cheaper installation costs than TCSC does, it is the FACTS device that provides the most value for the money.**

Keywords - FACTS,Deregulated market system,Security Constrained Optimal Power Flow,Bilateral Exchange.

I. INTRODUCTION

Since the population has been growing at an alarming rate over the past few years, electric utilities have been forced to maintain the integrity of their systems while also increasing the amount of power that is delivered through their networks [1]. As more people use electricity, the sector is shifting towards a deregulated structure in order to better serve the requirements of consumers. Pool, bilateral, and hybrid power systems are the three primary categories that fall under the category of deregulated power systems [2]. Examining SCOPF through the lens of a bilateral model of a deregulated electricity system is the focus of this paper. Transactions in a bilateral model are carried out directly between the two parties involved in the transaction. Customers and providers of electricity will be allowed to sign a wide variety of bilateral service contracts thanks to the deregulation of the industry [3]. When modelling bilateral transactions, secured bilateral transaction matrices that use AC distribution components with slack bus contribution are used [4, 5]. Synchronous generators are responsible for providing the reactive power for the pure bilateral arrangement with the reactive power.In the context of the operation of the electricity system, mixed physical bilateral transactions and pool-supplied demand, with varied degrees of combined pool-bilateral coordination, are being examined [6].

Increasing system performance by striking a balance between safety and efficiency is the goal of the Security Constrained Optimal Power Flow (SCOPF) methodology. The SCOPF is a particular instance of the OPF that takes into account restrictions brought about by the functioning of the system in accordance with a predetermined group of assumptions. The SCOPF problem has both continuous and discrete variables, which transforms it into a nonlinear, non-convex, huge optimisation problem [7, 8].

In order to solve this problem, either the existing transmission lines need to be utilised more effectively or new lines need to be installed. Both options are necessary. Because the expansion of the power transmission network is restricted by concerns about environmental right-of-way and expense, it is necessary to make more efficient use of the resources that are already available in the electrical grid. As a result of recent advancements in power electronics [9, 10], there has been a significant uptick in interest in Flexible AC Transmission Systems (FACTS) devices that can be utilised in transmission systems.

SCOPF with FACTS tools, employing both time-honoured methods and modern computational procedures. A sensitivity-based technique was devised to position the thyristor-controlled series compensator (TCSC) and the unified power flow controller (UPFC) [11], taking into consideration the system's voltage and angle sensitivities in relation to variations in the load. Continuation Power Flow (CPF) was utilised to assist in the sizing and positioning of the series compensators for the purpose of improving the overall system reliability and safety. The research identifies the optimal locations for series and shunt compensators and finds the values that are best suited to describe their parameters [12]. Using population-based computational intelligence methodologies like the Genetic Algorithm (GA), Evolutionary Programming (EP), and Particle Swarm Optimisation (PSO), the optimal location of FACTS devices was figured out. EP was created to achieve optimal placement of multi-type FACTS devices in order to optimise the overall transfer capability while simultaneously limiting the total system power loss [13]. This was done in order to improve upon the findings that were obtained by using the loss sensitivity index technique. PSO [14] determined the optimal placement for single-type and multi-type FACTS devices in order to improve the system's overall level of safety. DE is the easiest algorithm to use, the most trustworthy, and the one that is effective most consistently when compared to other algorithms that are used to tackle optimisation problems [15]. This research makes use of DE to determine where these components should be located and how their parameters should be created in order to secure optimal power flow in a bilateral model of a deregulated power system. This is done in order to obtain a secure, optimal power flow. This task is completed in two stages. The first thing that has to be done is to compile a safe bilateral transaction matrix that deviates from the specified matrix as little as is humanly practicable. After determining that the equality and inequality conditions are satisfied, the second step is to select the most suitable location for the TCSC and SVC in order to bring down the cost of active power generation and the cost of installing the FACTS devices. On an IEEE 6 bus system, simulations are executed, and the resulting data is reviewed in order to validate the claimed level of performance.

II.OBJECTIVE

A.To enhance Power Quality

B.To achieve Security Constrained optimal power flow in a deregulated power system

C.To reduce cost of installation of Flexible Alternating Current Transmission System

CIII. LITERATURE SURVEY

A highly doped NBL layer can be put in the junction of the N-epi and P-sub layers in order to further reduce the substrate leakage current when the device is operating in conduction mode. [16] Because the HV JFET is a majority carrier device, the equivalent reverse recovery feature of the bootstrap diode emulator is also competitive, and its implementation is qualitatively investigated. This is because the HV JFET is a majority carrier device.

The primary [17] contribution made by this research is a pair of tighter achievable and converse bounds for D2D coded caching. These bounds continue to be valid even in the presence of colluding users, which means that some users exchange cached contents and demand file indices. To begin, we recommend a D2D private caching technique, the primary component of which is the use of fake users to "hide" the actual users' needs from the system. This allows the system to more efficiently meet those needs. By comparing the feasible D2D private load with an existing converse bound for the shared-link model without demand privacy restriction, it is shown that the recommended technique is order-optimal, with the exception of the very low memory capacity regime when there are more files than users. This is the only regime in which the order optimality of the offered

approach cannot be shown. Second, a new achievable scheme and a new converse bound under the constraint of uncoded cache placement are developed for the case of two users and shown to be within a constant factor of one another for all system parameters. This sheds light on the open parameter regime. By introducing a cut-set type parameter, the converse bound that was designed for two users may be generalised to work for any number of users. This new converse binding demonstrates that the virtual user's technique is optimal across the board for all parameter regimes by utilising the limitations of uncoded cache placement and user cooperation as stipulations. As a consequence of this, the failure of the device in HV-TFTs is caused by the breakdown of the dielectric close to the end of the gated channel. This is in contrast to the failure of traditional TFTs, which is caused by the destruction of the semiconductor close to the drain. This research elucidates the reasons why HV-TFTs fail and proposes a practical design strategy for reaching a happy medium between the breakdown voltages of HV-TFTs and their on-currents. [18] Specifically, this research focuses on achieving a balance between the two. The capacity of a flexible alternating current transmission system (in this example, a static synchronous series compensator) to reduce grid current changes and, as a result, flicker is the primary subject of this body of research material. When there is a change in the wind speed, there is also a change in the mechanical torque, which has an influence on the grid current that is monitored by the static synchronous series compensator. The grid-connected technology has been subjected to a meticulous case-by-case analysis, during which both low and high wind speeds were taken into consideration. There have been instances in which the static synchronous series compensator has been utilised for the series voltage injection of both inductive and capacitive types. We are able to demonstrate, with the help of MATLAB and Simulink, that the proposed approach effectively lessens flicker by utilising a static synchronous series compensator for inductive series voltage injection. A method for real-time CM of semiconductors in modular multilevel converters (MMCs) is presented here. This method makes use of a hierarchy of cascading H-bridge modules. In order to ascertain whether or not a transition has taken place, the CM algorithm relies on monitoring the on-resistance of semiconductors over the course of time. [19] Using the method that was recommended, it was proved that successful curve tracing of semiconductors in MMCs is possible, with the semiconductor junction maintaining a temperature that can be easily detected despite enduring minute fluctuations. An estimate of the on-state resistance value can be derived using the observed arm current and the measured on-state voltage drop of the semiconductors as inputs. This yields an approximation of the on-state resistance value. One can differentiate the effects of those brought on by ageing from those brought on by variations in temperature if readings of the on-state resistance are taken at temperatures that are under control.

In order to solve the many-to-many CP-CR pairing problem, which is based on the proposed contract-based incentive mechanism, we also present a matching technique with polynomial complexity as a solution. The outcomes of the simulations provide evidence that our suggested method is effective in enticing user devices to take part in D2D computation offloading and in selecting the most suitable CPs to carry out the computation jobs for related CRs. This is demonstrated by the fact that we were able to select the most suitable CPs [20].

This [21] presents an in-depth study on self-heating effects, sometimes known as SHEs, in tree-FET devices operating at 5nm technology nodes. According to a comparison with the Nanosheet FET (NSFET), the Tree-FET, which consists of three channels and two bridges, is more analogous to a five-channel NSFET than it is to a three-channel NSFET. Evaluation of tree-FETs for use in future technological nodes based solely on the factor of rising ON current, as shown by a comprehensive physics-based analysis, is insufficient, as the study reveals. To demonstrate that Tree-FET is more dependable than competing technologies under self-heating conditions, which is of utmost relevance at lower technological nodes, numerical simulations are employed.

In light of these factors [22], the research presented here presents a device detection and identification architecture (DDI) that may be used for simultaneous identification of audio-visual (AUD) and Internet of Things (IoT) devices by making use of received overlay signals. The recovered Fourier patterns are used as the representative feature vector in the design. This was done so that the detecting and identifying process may be improved. Trials have shown that not only does the architecture have a lower computing complexity than standard schemes and techniques based on deep neural networks, but it also has a higher success probability for the AUD problem. This was discovered by analysing the results of the trials. An evaluation of the DDI architecture for IoT device identification tasks was carried out, and it was compared to a number of different shallow learning techniques in order to illustrate its utility even further.

The [23] of this article makes a suggestion for a remedy that relies on the development and use of a portable monitor for the patient's breathing rate. This programme will monitor this biometric variable and inform users when it goes outside of healthy parameters. At this point, a spirometry test may be necessary in order to discover the condition in its earlier stages, when it is most curable. In order to incorporate this instrumentation system, the framework of a pair of glasses will be altered so that the sensor can sit on the nasal platelets. This will allow the device to be worn.

[24] We use a well-orchestrated data augmentation technique to automatically construct adequate AATCs for different positions using a small quantity of obtained data in order to account for the differences in AATCs observed from different relative locations. This allows us to account for the variances in AATCs measured from different relative positions. Next, AATCs are utilised in the training process for the liquid detection model. We conduct exhaustive research on a significant number of high-profile instances of liquid fraud, and the results of our investigations demonstrate that we have an accuracy ranging from 92% to 97% when it comes to spotting the scam [25].

IV. SIMULATION OF DATA ELEMENTS

A. TCSC MODELLING

A thyristor-controlled series compensating capacitor, also known as a thyristor-controlled shunt capacitor (TCSC), is one that is bypassed by a thyristor-controlled reactor. It is modelled as a tunable reactance that is linked in series with the transmission line to regulate the impedance of the line and, as a result, the power flow in order to make the network safer. This is done in order to increase the network's overall safety.

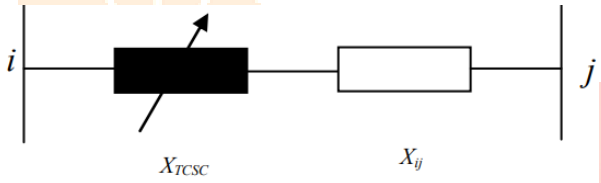

Fig. 1 Block diagram of TCSC

B. MODELLING OF SVC

As can be seen in Figure 2 [26], SVC is depicted as a shunt-connected static VAR generator or absorber that goes by the name QSVC. The output of this device has its value adjusted so that it can switch between capacitive and inductive compensation.

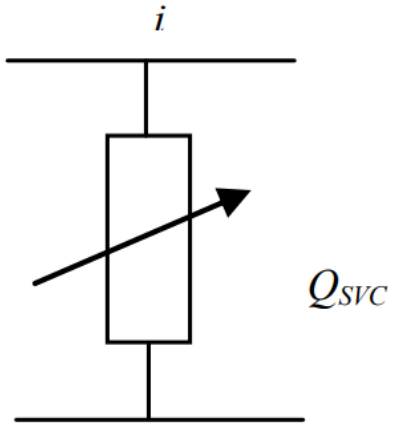

Fig. 2 Block diagram of SVC

C. THE CONSTRUCTION OF A GRID FOR SECURE BILATERAL TRANSACTIONS

A model of a lossless bilateral contract can be developed by treating the contracts as independent variables and the system security restrictions as fixed ones [9]. This will allow for the creation of the model. Some of the characteristics that are built into this transaction matrix are column rules, row rules, range rules, and flow rules [8, 9]. It is only possible to have trustworthy bilateral transactions between buyers and sellers if the transaction matrix satisfies all of its essential properties. Customers in a deregulated power system that uses a bilateral model have the ability to negotiate pricing and terms of service directly with

generators in order to secure the most favourable terms and rates. This concept is sometimes referred to as the direct access model. This is illustrated in Figure 3.

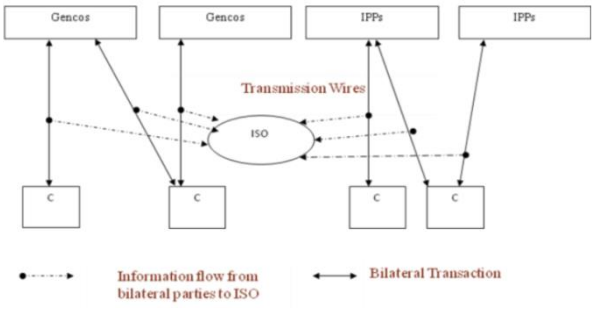

Fig.3. Bilateral Model of Deregulated Power System

V. RESULT AND DISCUSSIONS

Platforms for equipment and diagnostic testing MATLAB 2021a was used to write the DE code, and a modified version of MATLAB's power simulation tool, MATPOWER 4.0b4, was used to solve the SCOPF problem [27]. Validation of DE algorithms has been accomplished through the use of the IEEE's 6-bus test system. In TABLE I, we present an overview of the initial parameter configurations that are utilised by both the PSO and DE algorithms. The simulations are carried out using a computer that features a 2.66 GHz Intel i3 CPU and 4 gigabytes of random access memory (RAM).

Infrastructure for testing on the IEEE 6-bus The IEEE 6 bus system includes three generators, three power supplies, eleven transmission lines, and six buses in total. On a scale of one hundred MVA, the information regarding the system can be found. For the baseline scenario, we require 210 megawatts of actual power and 210 megavolt-ampere-seconds of reactive power.

The suggested bilateral transaction matrix is presented in Table II, and the secured bilateral transaction matrix is produced from the outcomes of the bilateral model and presented in Table III. Both matrices can be found at the same location.

It was determined whether or not optimal placement of FACTS devices had any impact on any of the four different scenarios.

- The SCOPF Ignoring Facts and Line Boundaries Is a First Example of This.
- SCOPF deciding to use line restrictions rather than facts
- The SCOPF and TCSC Have a Conversation About the Line Boundaries
- Taking into consideration the line limits for SCOPF

Parameters	**Values**
Population Size	20
Number of iterations	200
Number of variables	2
Scaling Factor	0.8
Crossover Ratio	0.8
Convergence criteria	10^{-6}

Value of transaction between generator and load bus (p.u)		
T(1,4)=0.2	T(1,5)=0.4	T(2,4)=0.4
T(3,4)=0.1	T(3,5)=0.3	T(3,6)=0.7

Value of transaction between generator and load bus (p.u)		
T(1,4)=0.1	T(1,5)=0.4	T(2,4)=0.1
T(3,4)=0.1	T(3,5)=0.3	T(3,6)=0.2

Generator Number	Bidding Cost
1	11 ($/Mwhr)
2	15 ($/Mwhr)
3	12 ($/Mwhr)

	Case 1	Case 2	Case 3	Case 4
Pg1	107.87 MW	60 MW	60 MW	60 MW
Pg2	50 MW	40.MW	40 MW	40 MW
Pg3	60MW	110MW	110 MW	40 MW

	Case 1	Case 2	Case 3	Case 4
Qg1	55.79 MVAR	15.95 MVAR	55.37 MVAR	79.84 MVAR
Qg2	46.21 MVAR	74.35 MVAR	43.71 MVAR	89.57 MVAR
Qg3	77.22 MVAR	89.62 MVAR	79.26 MVAR	100 MVAR

ESTIMATES OF THE COST OF AN IEEE 6-BUS SYSTEM

Table V contains the result of adding up three different measurements that represent the generators' real power output. According to the table, the actual amount of power generated by each of the three generators is within acceptable parameters. Figures relating to reactive power generation. According to the data, reactive power generation satisfies all of the limitations at all of the generators. Both the real power and the reactive power graphs are displayed down below.

The information that can be found in Table VII includes the cost of active power generation and the cost of installing FACTS devices, as well as the location of TCSC and SVC and the parameter values for both. The bid price is used to calculate the cost of generating active power, and this information may be found in Table IV. According to the findings of the DE algorithm, line 9 (3-6) is the best location for the TCSC since it has the lowest cost of active power generation at 2372.56 dollars per hour. Table VII contains this information for your perusal. In addition, the DE algorithm has identified the best configuration for the parameters of the TCSC, which has led to the production of active power at the lowest feasible cost. It indicates that DE can be achieved with benefits such as shorter calculation time and cheaper active power production if TCSC is placed in the best feasible location and its settings are adjusted. The proposed method has identified the optimal location for an SVC as well as the optimal way to provide the parameters of this component. By locating SVC in the optimal location (bus 5), we were able to reduce the cost of actively generating power from 2372.56 dollars per hour to 2370.25 dollars per hour. A comparison of the costs of active power generation, the installation of the FACTS device, and the overall cost.

By relocating TCSC to lines 3-6 with the acquired parameter setting, line 2-4 loading is decreased to 98.23%, as shown in Table VIII. Furthermore, by relocating SVC to bus line 5, line 2-4 loading is reduced to 84.48%.

VI. CONCLUSIONS

When it comes to the deregulated electricity market, there are a variety of approaches that can be utilised to handle power transmission network challenges without expanding the network itself due to concerns around the expense of environmental rights-of-way and cost. Normal operations and emergency operations both benefit from an increase in safety when a power system is equipped with TCSC and SVC devices. It is essential to their effectiveness that TCSC and SVC devices be placed in the appropriate locations. In this paper, the DE method was used to establish the ideal positions for the TCSC and SVC in relation to the SCOPF issue. The criterion for optimisation takes into account the cost of active power generation in addition to the cost of the TCSC and SVC installations. Throughout the simulations, the IEEE 694 bus test system was utilised. In light of the findings, it is abundantly obvious that DE is the best algorithm for solving the SCOPF problem posed by the optimal placement of FACTS devices in the transmission system under the Bilateral Model of the deregulated energy market. This problem was posed by the optimal deployment of FACTS devices in the transmission system. When compared to the other FACTS device that is used, the SVC has both reduced active power generation costs as well as lower installation expenses. In conclusion, DE with SVC offers higher performance when used to solve the SCOPF problem of optimally deploying FACTS devices in the transmission system in the bilateral model of a deregulated power system with FACTS devices utilising a computational intelligence algorithm. This problem arises in the context of the bilateral model of a deregulated power system with FACTS devices.

VII.SCOPE OF WORK

In future the problem of Security Constrained Optimal power flow can further be analysed and solved using other intelligent methods using Particle Swarm optimisation and Combination of Artifical Neural network and Fuzzy logic Technology as ANFIS.Further cost of optimsation of location of FACTS controller can be achieved using testing other IEEE buses and sampling the data.

VIII.REFERENCES

[1]. L. Benatti and F. M. Puglisi, "Impedance Investigation of MIFM Ferroelectric Tunnel Junction Using a Comprehensive Small-Signal Model," in IEEE Transactions on Device and Materials Reliability, vol. 22, no. 3, pp. 332-339, Sept. 2022.

[2]. P. Wu and J. Appenzeller, "Explaining Steep-Slope Switching in Carbon Nanotube Dirac-Source Field-Effect Transistors," in IEEE Transactions on Electron Devices, vol. 69, no. 9, pp. 5270-5275, Sept. 2022.

[3]. A. Althuwayb et al., "Metasurface-Inspired Flexible Wearable MIMO Antenna Array for Wireless Body Area Network Applications and Biomedical Telemetry Devices," in IEEE Access, vol. 11, pp. 1039-1056, 2023.

[4]. Z. Zhang, Y. Tian, R. Deng and J. Ma, "A Double-Benefit Moving Target Defense Against Cyber–Physical Attacks in Smart Grid," in IEEE Internet of Things Journal, vol. 9, no. 18, pp. 17912-17925, 15 Sept.15, 2022.

[5]. D. Cittanti, E. Vico and I. R. Bojoi, "New FOM-Based Performance Evaluation of 600/650 V SiC and GaN Semiconductors for Next-Generation EV Drives," in IEEE Access, vol. 10, pp. 51693-51707, 2022.

[6]. M. Emad-ud-din and Y. Wang, "Promoting Occupancy Detection Accuracy Using On-Device Lifelong Learning," in IEEE Sensors Journal.

[7]. S. Lee and D. H. Lee, "From Attack to Identification: MEMS Sensor Fingerprinting Using Acoustic Signals," in IEEE Internet of Things Journal, vol. 10, no. 6, pp. 5447-5460, 15 March15, 2023.

[8]. Z. Shi, J. A. Zhang, R. Y. Xu and Q. Cheng, "Environment-Robust Device-Free Human Activity Recognition With Channel-State-Information Enhancement and One-Shot Learning," in IEEE Transactions on Mobile Computing, vol. 21, no. 2, pp. 540-554, 1 Feb. 2022.

[9]. C. E. Staniloiu, A. Militaru, R. Nitu and R. Deaconescu, "Safer Linux Kernel Modules Using the D Programming Language," in IEEE Access, vol. 10, pp. 134502-134511, 2022.

[10]. Y. Zhang, B. Li, J. Wu, B. Liu, R. Chen and J. Chang, "Efficient and Privacy-Preserving Blockchain-Based Multifactor Device Authentication Protocol for Cross-Domain IIoT," in IEEE Internet of Things Journal, vol. 9, no. 22, pp. 22501-22515, 15 Nov.15, 2022.

[11]. X. Huang and S. Zhou, "Importance-Aware Data Pre-Processing and Device Scheduling for Multi-Channel Edge Learning," in Journal of Communications and Information Networks, vol. 7, no. 4, pp. 394-407, Dec. 2022.

[12]. Z. Zhang, R. Deng, Y. Tian, P. Cheng and J. Ma, "SPMA: Stealthy Physics-Manipulated Attack and Countermeasures in Cyber-Physical Smart Grid," in IEEE Transactions on Information Forensics and Security, vol. 18, pp. 581-596, 2023.

[13]. Taïk, Z. Mlika and S. Cherkaoui, "Data-Aware Device Scheduling for Federated Edge Learning," in IEEE Transactions on Cognitive Communications and Networking, vol. 8, no. 1, pp. 408-421, March 2022.

[14]. V. Satyamsetti, A. Michaelides, A. Hadjiantonis and T. Nicolaou, "A Novel Simple Inductor-Controlled VAR Compensator," in IEEE Transactions on Circuits and Systems II: Express Briefs, vol. 69, no. 2, pp. 524-528, Feb. 2022.

[15]. J. Wang, J. Tian, Y. Liu, D. Yang and T. Liu, "MMTD: Multi-stage Moving Target Defense for Security-enhanced D-FACTS Operation," in IEEE Internet of Things Journal.

[16]. Z. Yuan et al., "A Bootstrap Diode Emulator Integration to 600 V N-Type Epitaxial Platform for High Voltage Gate Driver IC," in IEEE Electron Device Letters, vol. 43, no. 11, pp. 1941-1944, Nov. 2022.

[17]. K. Wan, H. Sun, M. Ji, D. Tuninetti and G. Caire, "On the Fundamental Limits of Device-to-Device Private Caching Under Uncoded Cache Placement and User Collusion," in IEEE Transactions on Information Theory, vol. 68, no. 9, pp. 5701-5729, Sept. 2022.

[18]. X. Li et al., "Widely Adjusting the Breakdown Voltages of Kilo-Voltage Thin Film Transistors," in IEEE Electron Device Letters, vol. 43, no. 2, pp. 240-243, Feb. 2022.

[19]. Mishra and K. Chatterjee, "Flicker Attenuation Using FACTS Device for DFIG-Based WECS Connected to Distribution Network," in IEEE Systems Journal, vol. 17, no. 1, pp. 282-293, March 2023.

[20]. M. Asoodar, M. Nahalparvari, Y. Zhang, C. Danielsson, H. -P. Nee and F. Blaabjerg, "Accurate Condition Monitoring of Semiconductor Devices in Cascaded H-Bridge Modular Multilevel Converters," in IEEE Transactions on Power Electronics, vol. 38, no. 3, pp. 3870-3884, March 2023.

[21]. M. Chen, H. Wang, D. Han and X. Chu, "Signaling-Based Incentive Mechanism for D2D Computation Offloading," in IEEE Internet of Things Journal, vol. 9, no. 6, pp. 4639-4649, 15 March15, 2022.

[22]. S. Srivastava, M. Shashidhara and A. Acharya, "Investigation of Self-Heating Effect in Tree-FETs by Interbridging Stacked Nanosheets: A Reliability Perspective," in IEEE Transactions on Device and Materials Reliability, vol. 23, no. 1, pp. 58-63, March 2023.

[23]. K. Dev, S. A. Khowaja, P. K. Sharma, B. S. Chowdhry, S. Tanwar and G. Fortino, "DDI: A Novel Architecture for Joint Active User Detection and IoT Device Identification in Grant-Free NOMA Systems for 6G and Beyond Networks," in IEEE Internet of Things Journal, vol. 9, no. 4, pp. 2906-2917, 15 Feb.15, 2022.

[24]. M. Narducci and J. M. Aya, "Design of a wearable device for respiratory rate monitoring and detection of anomalous values," in IEEE Latin America Transactions, vol. 21, no. 3, pp. 513-518, March 2023.

[25]. Y. Yang, Y. Wang, J. Cao and J. Chen, "HearLiquid: Nonintrusive Liquid Fraud Detection Using Commodity Acoustic Devices," in IEEE Internet of Things Journal, vol. 9, no. 15, pp. 13582-13597, 1 Aug.1, 2022.

[26]. J. Zhang and F. Zhang, "Identity-Based Key Agreement for Blockchain-Powered Intelligent Edge," in IEEE Internet of Things Journal, vol. 9, no. 9, pp. 6688-6702, 1 May1, 2022.

[27]. K. M. J. Scheepens, N. Marsidi, R. E. Genders and T. Horeman-Franse, "The Compressiometer: Toward a New Skin Tensiometer for Research and Surgical Planning," in IEEE Journal of Translational Engineering in Health and Medicine, vol. 10, pp. 1-9, 2022, Art no. 2500109.